

# Rheological and Tribological Properties of Ionic Liquid-Based Nanofluids Containing Functionalized Multi-Walled Carbon Nanotubes

Baogang Wang,<sup>†,§</sup> Xiaobo Wang,<sup>†</sup> Wenjing Lou,<sup>\*,†</sup> and Jingcheng Hao<sup>\*,†,‡</sup>

State Key Laboratory of Solid Lubrication, Lanzhou Institute of Chemical Physics, Chinese Academy of Sciences, Lanzhou 730000, People's Republic of China, Key Laboratory of Colloid and Interface Chemistry, Shandong University, Ministry of Education, Jinan 250100, People's Republic of China, and Graduate School of Chinese Academy of Sciences, Beijing 100039, People's Republic of China

Received: January 19, 2010; Revised Manuscript Received: March 16, 2010

Room temperature ionic liquid-based nanofluids containing functionalized multi-walled carbon nanotubes (F-MWCNTs) were fabricated. Transmission electron microscopy (TEM), field emission scanning electron microscopy (FE-SEM), Fourier transform infrared (FT-IR), and X-ray photoelectron spectra revealed the morphology and chemical structure of the obtained F-MWCNTs. The rheological behaviors of the F-MWCNTs/1-butyl-3-methylimidazolium hexafluorophosphate ([Bmim][PF<sub>6</sub>]) nanofluids were studied, demonstrating the shear thinning behavior of nanofluids at rather low concentrations, which could be due to the high specific ratio, flexibility of F-MWCNTs, and the formation of a transient network through nanotube–nanotube and nanotube–matrix interactions. It was found that the rheological behavior of the F-MWCNTs (0.1 wt %)/[Bmim][PF<sub>6</sub>] nanofluid was similar to that of the surfactant worm-like micelle systems. Therefore, the transient network structure of the F-MWCNTs (0.1 wt %)/[Bmim][PF<sub>6</sub>] nanofluid could be renovated in a short time after shearing forces were input. The shear viscosity of the nanofluids was even lower than that of pure [Bmim][PF<sub>6</sub>], especially under high shear rates, which could be attributed to the self-lubrication of F-MWCNTs. The tribological properties of the nanofluids were also evaluated in comparison with those of pure [Bmim][PF<sub>6</sub>] under loads in the range of 200–800 N, indicating that the nanofluids exhibited preferable friction-reduction properties under 800 N and remarkable antiwear properties with use of reasonable concentrations.

## 1. Introduction

Carbon nanotubes (CNTs), both single- and multi-walled ones, have attracted tremendous attention since their discovery<sup>1</sup> because of their unique electronic and mechanical properties.<sup>2–4</sup> It has been reported that CNTs are extremely strong, and exceptionally stiff, yet remarkably flexible.<sup>5</sup> In addition, CNTs have high specific ratios<sup>6</sup> (>100) but low density. These properties make them excellent additives to improve the mechanical,<sup>7</sup> electronic,<sup>7</sup> tribological,<sup>8,9</sup> thermal,<sup>10,11</sup> and rheological<sup>12</sup> properties of the matrix. However, CNTs have a strong tendency to aggregate because of their nanosize and respective high surface energy,<sup>13</sup> which greatly limits their applications.

Ionic liquids (ILs) are promising electrolytes due to their large electrochemical windows and higher ionic conductivities.<sup>14</sup> Furthermore, the physicochemical properties of ILs including dissolving ability and solvent miscibility can be tuned by altering the cation, anion, and attached substituents.<sup>15</sup> Hence, ILs have great potential applications in sensors,<sup>16</sup> catalysis,<sup>14,15</sup> solar and fuel cells,<sup>17</sup> storage and efficient use of energy,<sup>17</sup> and the electrochemistry field.<sup>18</sup> As the hydrophilicity and hydrophobicity of ILs can easily be tuned by varying the cations and/or counteranions,<sup>19,20</sup> utilization of the tunable properties of the ILs in nanometer-sized materials could open a new way to control properties of the materials.<sup>21</sup> Recently, several studies on covalent modification of multi-walled carbon nanotubes

(MWCNTs) with imidazolium cation-based ILs which can improve the dispersibility of MWCNTs in these corresponding ILs successfully have been reported.<sup>22–24</sup> The IL-functionalized MWCNTs (F-MWCNTs) show good dispersion, switchable solubility in corresponding solvents including ILs,<sup>22,23</sup> high charge-transfer activity,<sup>25</sup> and high electronic conductivity.<sup>26</sup> ILs suspensions containing F-MWCNTs can be considered as “nanofluids” because of their favorable homogeneity and stability, which is expected to combine the advantages of CNTs and ILs.

The nanofluid pioneered by Choi et al.<sup>27</sup> is a liquid suspension of nanometer-sized solid particles and fibers, which has been the most promising means of meeting the requirements for efficient thermal equipment.<sup>28</sup> The thermal conductivity of the nanofluids is conspicuously higher than those of base fluids, such as water, oil, and ethylene glycol.<sup>29–31</sup> In the past decade, the works of the CNTs nanofluids focused on the enhancement of their thermal conductivity.<sup>10,31–35</sup> However, the reports on their rheological properties and other properties are few.<sup>33,36</sup>

In the present paper, based on the wide uses of both CNTs and ILs in various fields and their excellent properties,<sup>2–6,14,15</sup> we chose a commercially available IL, 1-butyl-3-methylimidazolium hexafluorophosphate ([Bmim][PF<sub>6</sub>]), as a base liquid and F-MWCNTs as nanoadditives to fabricate nanofluids. The effects of the concentration of F-MWCNTs and temperature on the rheological properties of the F-MWCNTs/[Bmim][PF<sub>6</sub>] nanofluids were studied in more detail. Moreover, the tribological properties of the F-MWCNTs/[Bmim][PF<sub>6</sub>] nanofluids were also evaluated in a wide range of loads, comparing with pure [Bmim][PF<sub>6</sub>] which has been considered as a perfect lubricant

\* To whom correspondence should be addressed. Phone: +86 531 88366074. Fax: +86 531 88366074. E-mail: jhao@sdu.edu.cn and wjlou@licp.ac.cn.

<sup>†</sup> Lanzhou Institute of Chemical Physics, Chinese Academy of Sciences.

<sup>§</sup> Graduate School of Chinese Academy of Sciences.

<sup>‡</sup> Shandong University.

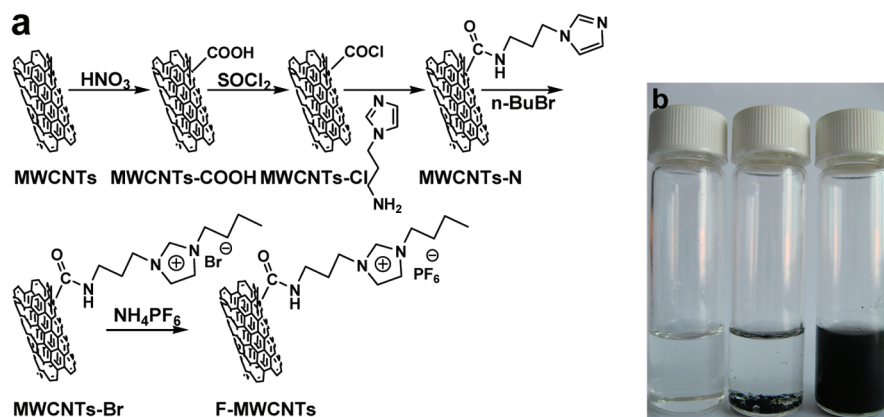


**Figure 1.** (a) Schematic procedures for synthesizing F-MWCNTs and (b) photos of pure [Bmim][PF<sub>6</sub>], [Bmim][PF<sub>6</sub>] suspensions of pristine MWCNTs, and F-MWCNTs (from left to right). The samples were equilibrated for 2 weeks after preparation.

since 2001.<sup>37</sup> The results reported here may open up new avenues for further investigation toward the applications of nanofluids.

## 2. Experimental Section

**2.1. Chemicals and Materials.** MWCNTs (diameter, 20–40 nm; length, 5–15  $\mu\text{m}$ ; purity,  $\geq 95\%$ ) prepared by chemical vapor deposition (CVD) were purchased from Shenzhen Nanotech Port Ltd., Co. (China) and 1-(3-aminopropyl)imidazole ( $\geq 98\%$ ) from Alfa Aesar. 1-Methylimidazole ( $\geq 98\%$ , Shanghai Chemicals, China) was distilled at reduced pressure before use. 1-Bromobutane (98%, Shanghai Chemicals, China) was washed three times with H<sub>2</sub>SO<sub>4</sub> (98%, Tianjin Chemicals, China) followed by distilled water until the pH of the water was 7.0, dried with anhydrous MgSO<sub>4</sub> (AR, Shanghai Chemicals, China) overnight, and distilled at reduced pressure. Other reagents (AR, Tianjin Chemicals, China) were used as received.

**2.2. Synthesis.** F-MWCNTs were synthesized following previously documented protocols, with several small modifications, illustrated in Figure 1a.<sup>23</sup> High-purity [Bmim][PF<sub>6</sub>] was synthesized according to reference methods.<sup>38</sup> Then homogeneous and stable F-MWCNTs/[Bmim][PF<sub>6</sub>] nanofluids were prepared through mixing the F-MWCNTs and [Bmim][PF<sub>6</sub>] and ultrasonication (40 kHz) for 20 min, which is illustrated in Figure 1b.

**2.3. Characterization and Measurements.** Fourier transformation infrared (FT-IR) spectra were recorded on an IFS 66v/S FTIR spectrometer (Bruker, Germany), using the KBr disk method. X-ray photoelectron spectroscopy (XPS) analysis was obtained on a PHI-5702 multifunctional XPS. Field emission scanning electron microscopy (FE-SEM) images were obtained on a JEOL JSM-6701F field emission scanning electron microscope. Transmission electron microscopy (TEM) analyses were conducted on a Hitachi Model H-600 electron microscope at an accelerating voltage of 100 kV.

Rheological measurements were carried out on a HAAKE RS6000 Rheometer (Germany) with a coaxial cylinder sensor system (Z41 Ti). In steady shear experiments, the shear rate was typically increased from 0.05 to 1000 s<sup>-1</sup> within 5 min. In oscillatory measurements, an amplitude sweep at a fixed frequency of 1 Hz was performed prior to the following frequency sweep in order to ensure the selected stress was in the linear viscoelastic region. In experiments aiming to see temperature influence, temperature was typically increased from 25 to 45 °C with the help of a cyclic water bath (Phoenix). After each temperature rise, the sample was allowed to equilibrate for an additional 5 min before measurements.

The tribological measurements were evaluated with an Optimol SRV-IV oscillating friction and wear tester in a ball-on-disk contact configuration. The upper test piece was a  $\phi$  10 mm GCr15 bearing steel (AISI-52100) ball, and the lower test piece was a  $\phi$  24.00 × 7.88 mm GCr15 bearing steel (AISI-52100) flat disk. All the tests were conducted at a frequency of 25 Hz, amplitude of 1 mm, and 20 min of test duration. Prior to the friction and wear test, two drops of the lubricant were introduced to the ball-disk contact area. The friction coefficient curve was recorded automatically with a chart attached to the SRV-IV test rig. The wear volumes were conducted by a MicroXAM 3D surface profilometer (ADE Phase-Shift).

## 3. Results and Discussion

**3.1. Characterization of F-MWCNTs.** F-MWCNTs were synthesized and characterized by TEM, FE-SEM, FT-IR, and XPS measurements. The morphology and tubular structure of the pristine MWCNTs and F-MWCNTs were observed by FE-SEM and TEM, which is shown in Figure 2. The observations from Figure 2 indicate that the covalent modification and anion exchange processes did not deteriorate the structural integrity of MWCNTs. Moreover, the F-MWCNT surfaces look more viscous than those of the pristine MWCNTs because of the covalent modification. Figure 3a shows the FT-IR spectra of pristine MWCNTs, MWCNTs-COOH, and F-MWCNTs. The peak at 1712 cm<sup>-1</sup> corresponding to C=O stretching vibrations of the carboxyl group is observed in the spectrum of MWCNTs-COOH, which shifts to 1636 cm<sup>-1</sup> attributed to C=O stretching vibrations and C=C asymmetric stretching vibrations<sup>39</sup> in the spectrum of F-MWCNTs. The peaks at 2921 and 2980 cm<sup>-1</sup> attributed to symmetric and asymmetric stretching vibrations of C—H and the characteristic peak at 840 cm<sup>-1</sup> corresponding to P—F stretching vibrations in the spectrum of F-MWCNTs demonstrate the F-MWCNTs were successfully prepared. The XPS full-scan spectrum of MWCNTs-Br and the high-resolution spectra of corresponding elements are shown in Figure 3b. The binding energies were corrected for specimen charging by referring to the C<sub>1s</sub> at 284.8 eV. The peaks of N<sub>1s</sub> (402.1 eV)<sup>40</sup> and Br<sub>3d</sub> (68.3 eV)<sup>41</sup> verify the attachment of imidazolium cation-based ILs, whereas the disappearance of Br<sub>3d</sub> peak and the appearance of P<sub>2p</sub> (136.8 eV)<sup>42</sup> and F<sub>1s</sub> (685.6 eV)<sup>42</sup> corresponding to PF<sub>6</sub><sup>-</sup> in Figure 3c prove the anion exchange between Br<sup>-</sup> and PF<sub>6</sub><sup>-</sup>.

**3.2. Rheological Behaviors of F-MWCNTs/[Bmim][PF<sub>6</sub>] Nanofluids.** Rheological measurements can provide more detailed information about the microstructure of the nanofluids. In our current study, both the steady shear and oscillatory

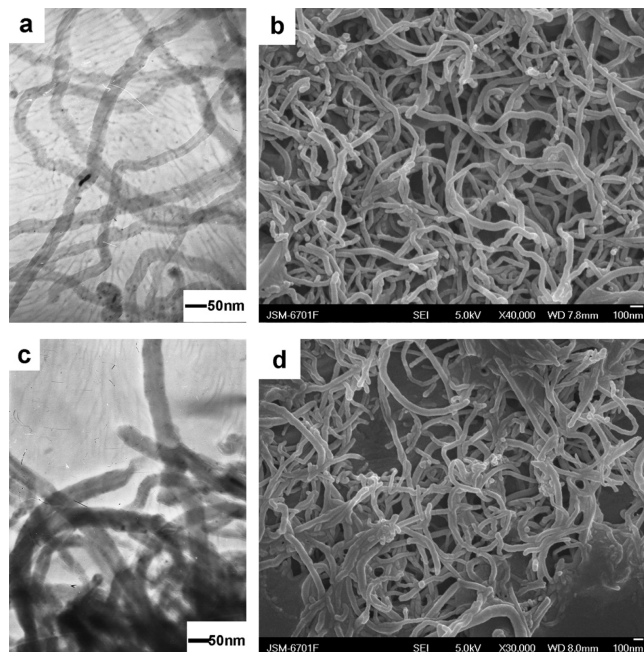


**Figure 2.** TEM images of pristine MWCNTs (a) and F-MWCNTs (c), and FE-SEM images of pristine MWCNTs (b) and F-MWCNTs (d).

measurements were first performed for the nanofluids of the F-MWCNTs/[Bmim][PF<sub>6</sub>] system. Figure 4a shows the influence of concentration on the shear viscosity of F-MWCNTs/[Bmim][PF<sub>6</sub>] nanofluids. As some imidazolium ILs can be well described as polymeric hydrogen-bonded supermolecules,<sup>43</sup> [Bmim][PF<sub>6</sub>] could be considered as a “structural” liquid rather than a simple liquid. Thus the nanofluids at low concentrations ( $\leq 0.04$  wt %) show a shear thinning behavior at low shear rate but Newtonian property at high shear rate, which may reflect the characteristic of the pure [Bmim][PF<sub>6</sub>].<sup>44</sup> When  $0.06 \leq c \leq 0.1$  wt %, the shear thinning property in a wide shear rate range shows a distinctly non-Newtonian behavior, indicating the transient network is formed through nanotube–nanotube and nanotube–matrix interactions. Furthermore, the shear viscosity of these nanofluids is lower than the viscosity of pure [Bmim][PF<sub>6</sub>] at much higher shear rate, which can be attributed to the self-lubrication of nanotubes.

As shown in Figure 4b, the complex viscosity of F-MWCNTs/[Bmim][PF<sub>6</sub>] nanofluids slightly increases with the increment of concentrations when  $c \leq 0.08$  wt %, while a relatively sharp increment of the complex viscosity for the F-MWCNTs (0.1 wt %)/[Bmim][PF<sub>6</sub>] nanofluid appears, verifying the nanofluid has elastic properties. The F-MWCNTs (0.1 wt %)/[Bmim][PF<sub>6</sub>] nanofluid in Figure 4a exhibits slight shear thickening at low shear rates while shear thinning above a critical shear rate, being highly viscous but also elastic due to the existence of a stably transient network. All these features are similar to the rheological behaviors of the cationic and anionic (catanionic) worm-like micelles systems.<sup>45</sup> Therefore, the F-MWCNTs in F-MWCNTs (0.1 wt %)/[Bmim][PF<sub>6</sub>] nanofluid can be seen as surfactant worm-like micelles because of their high specific ratio and flexibility. The different behaviors at low and high shear rates could be attributed to the further aggregation and entanglement of F-MWCNTs at low shear rates, and deformation and alignment at high shear rates.<sup>46</sup> More interesting phenomena of the F-MWCNTs (0.1 wt %)/[Bmim][PF<sub>6</sub>] nanofluid are investigated further in the following section.

Figure 5 shows the modulus of pure [Bmim][PF<sub>6</sub>] and the F-MWCNTs (0.1 wt %)/[Bmim][PF<sub>6</sub>] nanofluid as a function

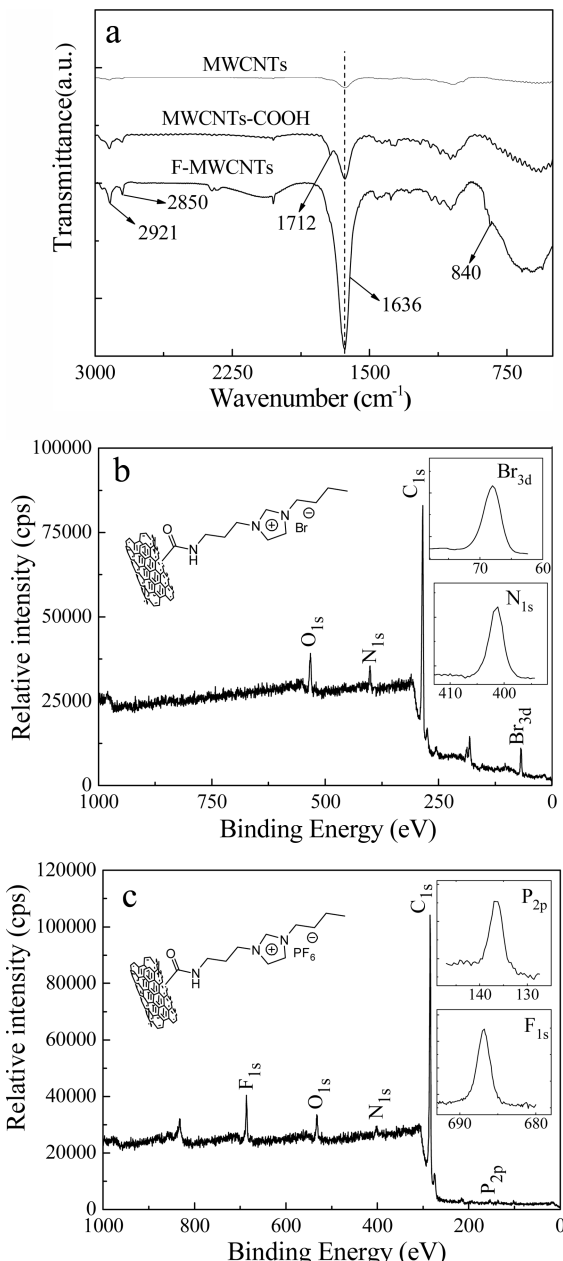


**Figure 3.** (a) FT-IR spectra of pristine MWCNTs, MWCNTs-COOH, and F-MWCNTs, and XPS full-scan spectra of MWCNTs-Br (b) and F-MWCNTs (c). Insets show the high-resolution spectra of corresponding elements.

of angular frequency.  $G''$  is always larger than  $G'$  over the whole frequency range, and  $G''$  and  $G'$  also follow a scaling law with exponents of 1 and 1.36, respectively, which is a typical rheological feature of a polymer melt or solution.<sup>47</sup> The result is also similar to the observation in aqueous single-walled CNT suspensions, when the CNT concentration is below the critical “entangled” concentration.<sup>48</sup> In comparison with those of the pure [Bmim][PF<sub>6</sub>],  $G'$  of the nanofluid is increased to some extent with the increment of the angular frequency while there is no obvious variation for  $G''$ . Moreover,  $G''$  has an inflection point at a critical angular frequency, which could be attributed to the destruction of the ordered structure existing in pure [Bmim][PF<sub>6</sub>] or the nanofluid.

The viscoelastic behavior of the worm-like micelles is known to be reminiscent of that of “living” polymers and can be described by a model developed by Cates and co-workers.<sup>49,50</sup>

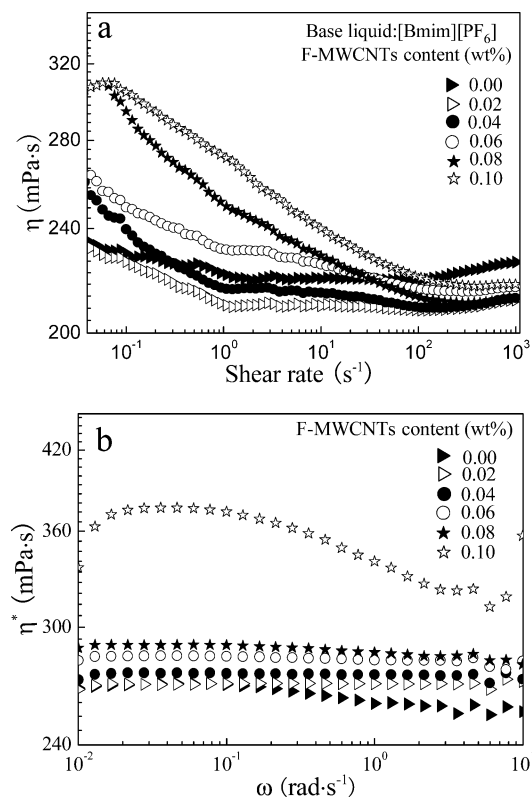


**Figure 4.** (a) Steady shear viscosity as a function of shear rate and (b) oscillatory complex viscosity as a function of angular frequency for F-MWCNTs/[Bmim][PF<sub>6</sub>] nanofluids with different concentrations.

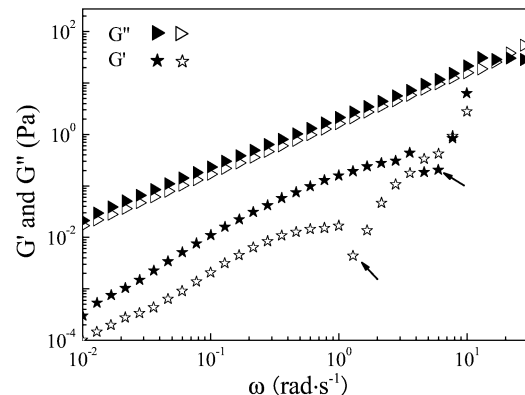


**Figure 5.** Storage modulus ( $G'$ ) and loss modulus ( $G''$ ) as a function of angular frequency for pure [Bmim][PF<sub>6</sub>] (empty symbols) and the F-MWCNTs (0.1 wt %)/[Bmim][PF<sub>6</sub>] nanofluid (solid symbols).

This model involves two relevant time scales: the reptation time  $\tau_{\text{rep}}$  and the breaking time  $\tau_{\text{break}}$ . If  $\tau_{\text{break}} \ll \tau_{\text{rep}}$ , chain breakage and recombination will both occur often. The “memory” property of the F-MWCNTs (0.1 wt %)/[Bmim][PF<sub>6</sub>] nanofluid was found in Figure 6. The shear viscosity curves of the nanofluid at various temperatures all show a similar shear thinning behavior, which indicates that the recombination of the transient network occurs during the equilibrium time after each temperature rise and shear measurement. Moreover, Figure 6 also shows that the shear viscosity of pure [Bmim][PF<sub>6</sub>] and the F-MWCNTs (0.1 wt %)/[Bmim][PF<sub>6</sub>] nanofluid both exhibit a dramatic reduction tendency with the increment of temperature.

**3.3. Tribological Properties of F-MWCNTs/[Bmim][PF<sub>6</sub>] Nanofluids.** The pure [Bmim][PF<sub>6</sub>] itself shows good tribological performance and has a potential application as a basic lubricant. So the tribological properties of various samples

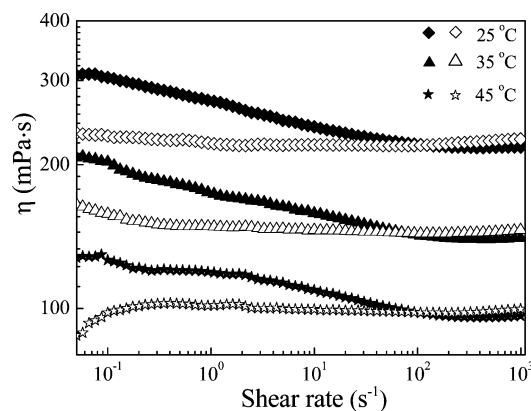


**Figure 6.** The steady shear viscosity of pure [Bmim][PF<sub>6</sub>] (empty symbols) and F-MWCNTs (0.1 wt %)/[Bmim][PF<sub>6</sub>] nanofluid (solid symbols) as a function of shear rate at various temperatures.

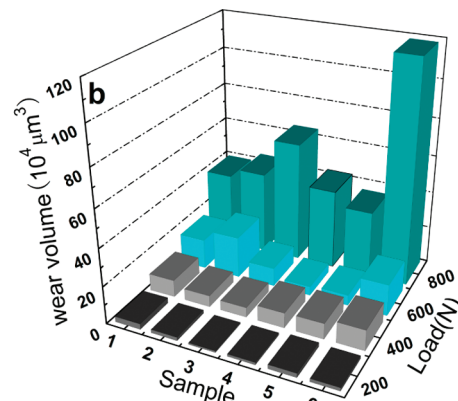
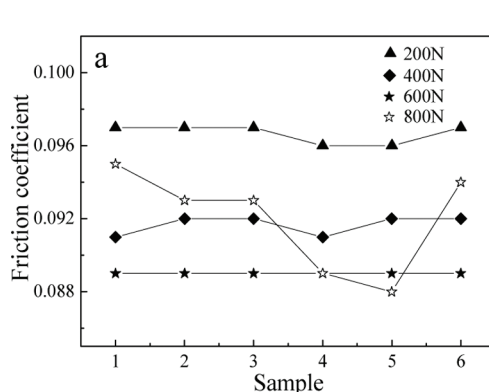
**TABLE 1: The Components of Various Samples Used for Tribological Measurements**

sample no.	base liquid	additives (wt %)
1	[Bmim][PF <sub>6</sub> ]	
2	[Bmim][PF <sub>6</sub> ]	F-MWCNTs (0.01)
3	[Bmim][PF <sub>6</sub> ]	F-MWCNTs (0.02)
4	[Bmim][PF <sub>6</sub> ]	F-MWCNTs (0.04)
5	[Bmim][PF <sub>6</sub> ]	F-MWCNTs (0.06)
6	[Bmim][PF <sub>6</sub> ]	pristine MWCNTs (0.01)

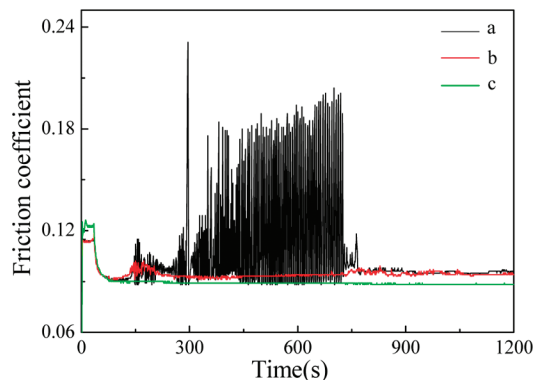
shown in Table 1 were evaluated and compared by using an optimal SRV-IV oscillating friction and wear test in order to study the influence of the pristine MWCNTs or F-MWCNTs as additives.

Figure 7 shows the friction coefficients and wear volumes of steel discs under various loads for different lubricating systems. No obvious difference for the friction coefficients of various samples was observed in Figure 7a due to the good lubrication properties of pure [Bmim][PF<sub>6</sub>] except under the load of 800 N. When compared with pure [Bmim][PF<sub>6</sub>] (sample 1) and sample 6 in Table 1, the F-MWCNTs/[Bmim][PF<sub>6</sub>] nanofluids (samples 2, 3, 4, and 5 in Table 1) with specific concentrations also exhibit obvious antiwear ability as lubricants under loads in the range of 200–800 N (shown in Figure 7b). The F-MWCNTs might play the role of roller bearing and separate the ball-disk contacts during the friction process under the load of 200 and 400 N.<sup>9</sup> Thus the adhesive wear was inhibited and the nanofluid with the lower concentration (sample 2 in Table 1) exhibits preferable antiwear ability, while the F-MWCNTs might first fill up the microgap of the rubbing surface and deposit there to form a self-assembly thin film that could provide protection for the surface from serious wear under the loads of 600 and 800 N.<sup>51</sup> Therefore, the nanofluids with relatively high concentrations (samples 4 and 5 in Table 1) are helpful to form the self-assembly thin films and exhibit better antiwear ability and friction-reduction properties (shown in Figure 7a) under rather high loads; otherwise, the integrity of the layer structure film of the IL<sup>52</sup> on the specimen will be destroyed by the F-MWCNTs<sup>53</sup> and the abrasive wear occurs.

Friction coefficient curves lubricated by various samples as a function of time under the load of 800 N are shown in Figure 8. The friction coefficients lubricated by sample 6 in Table 1 (Figure 8a) fiercely fluctuate with time at first during the friction process, which indicates that serious abrasive wear occurs due to the poor dispersibility of pristine MWCNTs. This phenomenon corresponds to the large wear volume lubricated by sample 6 under high loads (shown in Figure 7b), while the friction



**Figure 7.** Friction coefficients (a) and wear volumes of steel discs (b) lubricated by various samples in Table 1 under different applied loads.



**Figure 8.** Friction coefficient curves lubricated by (a) sample 6, (b) sample 1, and (c) sample 5 as a function of time under the load of 800 N at room temperature.

coefficient curve of the nanofluid (sample 5 in Table 1) shown in Figure 8c is smoother and lower than that of pure [Bmim][PF<sub>6</sub>] shown in Figure 8b, showing obvious friction-reduction properties.

To sum up, as an additive, the dispersity of the CNTs is a key factor to improve the tribological properties of pure [Bmim][PF<sub>6</sub>]. Therefore, the nanofluid (sample 5 in Table 1) exhibits remarkable friction-reduction properties under a load of 800 N compared to sample 6 in Table 1 and pure [Bmim][PF<sub>6</sub>]. Moreover, the antiwear ability of the pure [Bmim][PF<sub>6</sub>] with reasonable concentrations of F-MWCNTs as additives is improved under loads in the range of 200–800 N, which can be ascribed to the good dispersity of F-MWCNTs in [Bmim][PF<sub>6</sub>] and their superior mechanical properties.

#### 4. Conclusions

In conclusion, the F-MWCNTs/[Bmim][PF<sub>6</sub>] nanofluids were fabricated and their rheological and tribological properties were investigated in more detail. The rheological measurements exhibited a shear thinning behavior at rather low concentrations, which indicated that a transient network was formed through the nanotube–nanotube and nanotube–matrix interactions. The shear viscosity of the nanofluids was lower than [Bmim][PF<sub>6</sub>] especially under high shear rates. This phenomenon could be attributed to the self-lubrication of MWCNTs. The rheological behaviors of the F-MWCNTs (0.1 wt %)/[Bmim][PF<sub>6</sub>] nanofluid were similar to those of the worm-like micelles systems. Therefore, its network could recombine in a short time after shear measurements. Moreover, we also evaluated the tribological properties of the nanofluids and found that the nanofluids with reasonable concentrations showed obvious friction-reduc-

tion under 800 N and remarkable antiwear properties under loads in the range of 200–800 N compared to pure [Bmim][PF<sub>6</sub>]. The new applications of nanofluids still need to be further exploited, while the interesting rheological phenomena and tribological properties of the F-MWCNTs/[Bmim][PF<sub>6</sub>] nanofluids reported here are expected to supply fundamental data for their potential applications.

**Acknowledgment.** This work was supported by the NFSC (Grant No. 20803087), the Major State Basic Research Development Program of China (973 Program) (Grant No. 2007CB607606), and the Knowledge Innovation Program of the Chinese Academy of Sciences.

#### References and Notes

- Iijima, S. *Nature* **1991**, *354*, 56.
- Baughman, R. H.; Zakhidov, A. A.; de Heer, W. A. *Science* **2002**, *297*, 787.
- Thostenson, E. T.; Ren, Z. F.; Chou, T.-W. *Compos. Sci. Technol.* **2001**, *61*, 1899.
- Kongkanand, A.; Kamat, P. V. *ACS Nano* **2007**, *1*, 13.
- Salvetat, J.-P.; Bonard, J.-M.; Thomson, N. H.; Kulik, A. J.; Forró, L.; Benoit, W.; Zuppiroli, L. *Appl. Phys. A: Mater. Sci. Process.* **1999**, *69*, 255.
- Subramoney, S. *Adv. Mater.* **1998**, *10*, 1157.
- Moniruzzaman, M.; Sahin, A.; Winey, K. I. *Carbon* **2009**, *47*, 645.
- Peng, Y. T.; Hu, Y. Z.; Wang, H. *Tribol. Lett.* **2007**, *25*, 247.
- Yu, B.; Liu, Z. L.; Zhou, F.; Liu, W. M.; Liang, Y. M. *Mater. Lett.* **2008**, *62*, 2967.
- Choi, S. U. S.; Zhang, Z. G.; Yu, W.; Lockwood, F. E.; Grulke, E. A. *Appl. Phys. Lett.* **2001**, *79*, 2252.
- Jha, N.; Ramaprabhu, S. *J. Phys. Chem. C* **2006**, *112*, 9315.
- Bose, S.; Mukherjee, M.; Das, C. K.; Saxena, A. K. *J. Nanosci. Nanotechnol.* **2009**, *9*, 6569.
- Tasis, D.; Tagmatarchis, N.; Bianco, A.; Prato, M. *Chem. Rev.* **2006**, *106*, 1105.
- Părvulescu, V. I.; Hardacre, C. *Chem. Rev.* **2007**, *107*, 2615.
- van Rantwijk, F.; Sheldon, R. A. *Chem. Rev.* **2007**, *107*, 2757.
- Chen, H. J.; Wang, Y. L.; Liu, Y.; Wang, Y. Z.; Qi, L.; Dong, S. *J. Electrochem. Commun.* **2007**, *9*, 469.
- Wishart, J. F. *Energy Environ. Sci.* **2009**, *2*, 956.
- Li, Y. N.; Yang, J.; Wu, R. *Electrochim. Commun.* **2005**, *7*, 1105.
- Bonhôte, P.; Dias, A.-P.; Papageorgiou, N.; Kalyanasundaram, K.; Grätzel, M. *Inorg. Chem.* **1996**, *35*, 1168.
- Swatloski, R. P.; Visser, A. E.; Reichert, W. M.; Broker, G. A.; Farina, L. M.; Holbrey, J. D.; Rogers, R. D. *Green Chem.* **2002**, *4*, 81.
- Itoh, H.; Naka, K.; Chujo, Y. *J. Am. Chem. Soc.* **2004**, *126*, 3026.
- Yu, B.; Zhou, F.; Liu, G.; Liang, Y. M.; Huck, W. T. S.; Liu, W. M. *Chem. Commun.* **2006**, 2356.
- Park, M. J.; Lee, J. K.; Lee, B. S.; Lee, Y. W.; Choi, I. S.; Lee, S. *Chem. Mater.* **2006**, *18*, 1546.
- Wang, Z. J.; Zhang, Q. X.; Kuehner, D.; Xu, X. Y.; Ivaska, A.; Niu, L. *Carbon* **2008**, *46*, 1687.
- Zhang, Y. J.; Shen, Y. F.; Yuan, J. H.; Han, D. X.; Wang, Z. J.; Zhang, Q. X.; Niu, L. *Angew. Chem., Int. Ed.* **2006**, *45*, 5867.
- Zhao, F.; Wu, X. E.; Wang, M. K.; Liu, Y.; Gao, L. X.; Dong, S. *Anal. Chem.* **2004**, *76*, 4960.

- (27) Lee, S.; Choi, S. U. S.; Li, S.; Eastman, J. A. *J. Heat Transfer* **1999**, *121*, 280.
- (28) Prasher, R.; Phelan, P. E.; Bhattacharya, P. *Nano Lett.* **2006**, *6*, 1529.
- (29) Zhu, H. T.; Zhang, C. Y.; Tang, Y. M.; Wang, J. X. *J. Phys. Chem. C* **2007**, *111*, 1646.
- (30) Patel, H. E.; Das, S. K.; Sundararajan, T.; Nair, A. S.; George, B.; Pradeep, T. *Appl. Phys. Lett.* **2003**, *83*, 2931.
- (31) Wensel, J.; Wright, B.; Thomas, D.; Douglas, W.; Mannhalter, B.; Cross, W.; Hong, H. P.; Kellar, J.; Smith, P.; Roy, W. *Appl. Phys. Lett.* **2008**, *92*, 023110.
- (32) Xie, H. Q.; Lee, H.; Youn, W.; Choi, M. *J. Appl. Phys.* **2003**, *94*, 4967.
- (33) Yang, Y.; Grulke, E. A.; Zhang, Z. G.; Wu, G. F. *J. Appl. Phys.* **2006**, *99*, 114307.
- (34) Han, Z. H.; Yang, B.; Kim, S. H.; Zachariah, M. R. *Nanotechnology* **2007**, *18*, 105701.
- (35) Amrollahi, A.; Hamidi, A. A.; Rashidi, A. M. *Nanotechnology* **2008**, *19*, 315701.
- (36) Scarselli, M.; Scilletta, C.; Tombolini, F.; Castrucci, P.; Diociaiuti, M.; Casciardi, S.; Gatto, E.; Venanzi, A.; De Crescenzi, M. *J. Phys. Chem. C* **2009**, *113*, 5860.
- (37) Ye, C. F.; Liu, W. M.; Chen, Y. X.; Yu, L. G. *Chem. Commun.* **2001**, 2244.
- (38) Huddleston, J. G.; Visser, A. E.; Reichert, W. M.; Willauer, H. D.; Broker, G. A.; Rogers, R. D. *Green Chem.* **2001**, *3*, 156.
- (39) Jiang, H. J.; Zhu, L. B.; Moon, K. S.; Wong, C. P. *Carbon* **2007**, *45*, 655.
- (40) Everhart, D. S.; Reilley, C. N. *Surf. Interface Anal.* **1981**, *3*, 126.
- (41) Armstrong, J. E.; Walton, R. A. *Inorg. Chem.* **1983**, *22*, 1545.
- (42) Brant, P.; Benner, L. S.; Balch, A. L. *Inorg. Chem.* **1979**, *18*, 3422.
- (43) Dupont, J. *J. Braz. Chem. Soc.* **2004**, *15*, 341.
- (44) Kuang, Q. L.; Zhao, J. C.; Niu, Y. H.; Zhang, J.; Wang, Z. G. *J. Phys. Chem. B* **2008**, *112*, 10234.
- (45) Li, H. G.; Hao, J. C. *J. Phys. Chem. B* **2008**, *112*, 10497.
- (46) Karlson, L.; Nilsson, S.; Thuresson, K. *Colloid Polym. Sci.* **1999**, *277*, 798.
- (47) Ferry, J. D. In *Viscoelastic Properties of Polymers*; Wiley: New York, 1980.
- (48) Potschke, P.; Fornes, T. D.; Paul, D. R. *Polymer* **2002**, *43*, 3247.
- (49) Cates, M. E. *Macromolecules* **1987**, *20*, 2289.
- (50) Drye, T. J.; Cates, M. E. *J. Chem. Phys.* **1992**, *96*, 1367.
- (51) Pei, X. W.; Xia, Y. Q.; Liu, W. M.; Yu, B.; Hao, J. C. *J. Polym. Sci., Part A: Polym. Chem.* **2008**, *46*, 7225.
- (52) Liu, X. Q.; Zhou, F.; Liang, Y. M.; Liu, W. M. *Wear* **2006**, *261*, 1174.
- (53) Jiang, W. Q.; Yu, B.; Liu, W. M.; Hao, J. C. *Langmuir* **2007**, *23*, 8549.

JP1005346